

Protein Crystallization Induced by a Localized Voltage

Zoubida Hammadi, Jean-Pierre Astier, Roger Morin, and Stéphane Veesler*

Centre de Recherche en Matière Condensée et Nanosciences, CRMCN–CNRS, Universities Aix-Marseille II and III, Campus de Luminy, Case 913, F-13288 Marseille Cedex 09, France

Received January 30, 2007; Revised Manuscript Received May 23, 2007

ABSTRACT: In this paper, we present a new experimental setup for in situ investigation of the effect of a localized voltage on the nucleation and growth of proteins in the metastable zone. Our setup uses a crystallization cell in which one of the electrodes is sharp; because of the nanometer size of the tip, large electric fields, a large field gradient, and a high current density inside the solution are encountered near the tip, and depending on its polarity, we expect nucleation near the tip. Preliminary results indicate that this setup takes us closer to controlling the nucleation frequency and nucleation location. In this study, we address the unpredictability of the location of the critical nucleus. We expect that with the control of this location, we will be able to better understand the critical nuclei formation.

1. Introduction

Biophysical studies require structural information on the biomolecules studied and X-ray diffraction is the most powerful tool for this structural determination. Thus, the first step, sometimes called the bottleneck step, is the growth from solution of protein crystals suitable for X-ray diffraction studies. In crystallization from solution, there are at least two different successive problems to solve. First, after crystallization conditions have been determined, the nucleation rate must be controlled in order to obtain only a few high-quality single crystals near the equilibrium state, thus controlling growth. This latter task is extremely challenging. To avoid uncontrolled nucleation and because primary nucleation is a stochastic phenomenon, researchers often use seeding techniques.¹ An alternative solution is to induce crystallization from metastable solutions, in which nucleation does not occur, using an external magnetic,^{2,3} electric,^{4–6} ultrasonic,⁷ or electromagnetic^{8–15} field. Recently, the effects of an internal electric field on the crystallization of lysozyme were presented.⁶ The authors applied a direct current to 2 parallel 0.2 mm diameter Pt electrodes in contact with the protein solution. They observed (1) a preferential nucleation at the cathode and an amorphous phase at the anode, (2) that the number of crystals was lower than in absence of electric field, and (3) that the induction time of nucleation was decreased.

In this paper, in contrast with previous work,⁶ we present a new experimental setup for in situ investigation of the effect of a localized voltage on the nucleation and growth of lysozyme and bovine pancreatic trypsin inhibitor (BPTI) in the metastable zone. Our setup uses a crystallization cell where at least one of the electrodes is a sharp tip. Because of the nanometer size of the tip, large electric fields and a large field gradient are encountered near the tip. This geometry also induces a high current density inside the solution close to the region of high curvature. Depending on its polarity, we expect nucleation near the tip. Preliminary results indicate that this setup takes us closer to controlling the nucleation frequency and the nucleation location.

2. Materials and Methods

2.1. Materials. Hen-egg white lysozyme (14 600 Da, pI = 11.2) was purchased from Sigma (lot 89F 8276 L 6826) and used without

further purification. BPTI (6511 Da, pI = 10.5), was supplied as a lyophilized powder by Bayer and used as received. The purity of both proteins was checked by molecular sieving. Proper amounts of BPTI or Lysozyme and NaCl were dissolved in pure water (ELGA UHQ reverse osmosis system) to obtain stock solutions needed for crystallization experiments. The different solutions were buffered with 80 mM acetic acid, adjusted to pH 4.5 with NaOH (1 M), and filtered through 0.22 μm Millipore filters. The pH was checked with a pHmeter Tacussel ISIS 20000 equipped with a micro pH electrodes radiometer pHC3359-8. Lysozyme and BPTI concentrations were controlled by optical density measurements (Kontron UVKON810) using an extinction coefficient of 2.64 mL cm⁻¹ mg⁻¹ and 0.786 cm⁻¹ mL mg⁻¹¹⁶ at 280 nm for lysozyme and BPTI, respectively.

2.2. Methods. All experiments were performed in a glass vessel inserted in a thermostated cell under an optical microscope (Nikon Diaphot); the whole setup is shown in Figure 1.

We made the electrode from tungsten (W) wires (125 μm diameter) consisting of a sharp metallic tip emerging from the end of a glass capillary. First, a tungsten polycrystalline wire is placed inside a glass tube; the internal and external diameters of the tube are 300 μm and 1 mm, respectively. Second, electrical connections are made to the electrodes. Finally, the tip is fabricated by electrolytic etching in a 2 M NaOH solution (for a more detailed description, see the literature^{17,18}).

For experiments with BPTI, the electrodes were sharp (Figure 2), and for those with lysozyme, one was sharp and the other was rounded. The distance between the electrodes was roughly 600 μm . The electrodes were placed near the bottom of the crystallization cell.

Six hundred microliters of a supersaturated but metastable protein solution (no nucleation is observed within 24 h in absence of electric field) was placed in a 10 mm diameter glass vessel; an upper layer of 400 μL of inert paraffin oil (Hampton Research HR3-42) was added to avoid evaporation during the experiments. In all the experiments, direct voltage was applied to the electrodes (Metrix, Mtx 3240).

It is noteworthy that all the experimental solutions of this study are in the metastable zone for nucleation under normal conditions, that is, without any external perturbation.

3. Results and Discussion

In all the experiments conducted with a direct voltage in this study, we observed a decrease in nucleation time, an increase in growth kinetics, and often a predetermined positioning of the crystals. As previously shown by Nieto-Mendoza et al.¹⁹ and by our pH monitoring during some experiments, pH did not change enough to affect solubility (for one experiment, an ethanol mixture of methyl-orange was added to the protein solution and no change in color was observed). In the literature, the directed crystallization of proteins in an electric field is attributed to electromigration. Because in this work BPTI and

* Corresponding author. Phone: 336 6292 2866. Fax: 334 9141 8916. E-mail: veesler@crmcn.univ-mrs.fr.

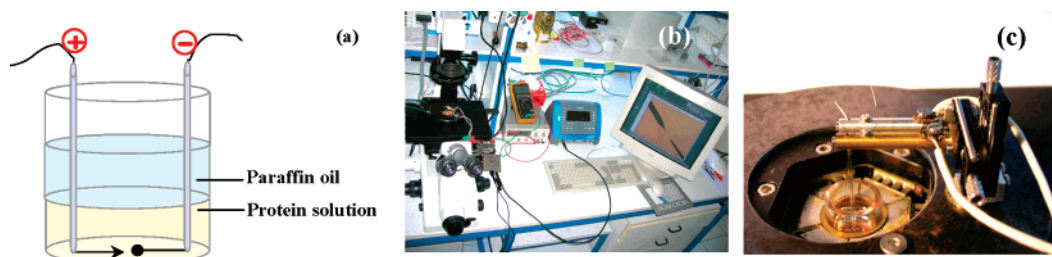


Figure 1. (a) Scheme of the crystallization cell with the two electrodes, (b) image of the whole experimental setup, and (c) *Y,Z* positioning stage for the electrodes.

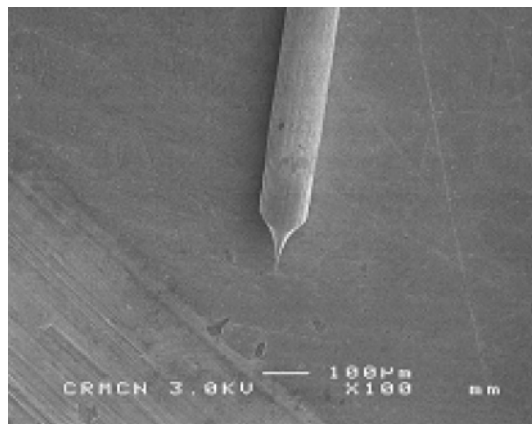


Figure 2. Scanning electron microscopy (JEOL 6320F) image of the tip of the sharp electrode.

lysozyme are positively charged at pH 4.5, we expected to observe crystallization at the cathode.

In addition, bubbles due to water electrolysis are formed at voltage values higher than 1 V. For this reason, we applied a constant direct voltage of 0.7–0.9 V, producing a current between 1 and 20 μA depending on the tip geometry and not on the distance between the electrodes.

The current was monitored during the experiments, showing a decrease of 1 order of magnitude within 10 min. During the experimental time (12–36 h), no bubbles were observed. Note that reproducibility was ensured by working at constant initial current

3.1. BPTI. Two sets of experiments were conducted for BPTI, denoted in the text as experiments 1 and 2.

Experiment 1: BPTI 20 mg/mL in 1.65 M NaCl and 80 mM sodium acetate buffer solution at pH 4.5, whose supersaturation corresponds to $\beta = 1.7$. Supersaturation β is defined as the ratio of the protein concentration in solution versus the solubility of the protein.¹⁶

We applied a direct voltage of 0.785 V and initial current $I_i = 28\mu\text{A}$, which was decrease to 2 μA within 15 min, $t_N < 1$ h and $t_{\text{exp}} = 20$ h, with t_N and t_{exp} corresponding to the induction time and experimental time, respectively.

In experiment 1, summarized in Figures 3 and 4, nucleation is enhanced and higher near the anode and crystals grow larger near the anode because of a concentration gradient between the electrodes. Moreover, a layer of what Moreno and Sasaki⁶ called amorphous precipitation is observed around the anode (Figures 3d and 4b).

To reduce the total number of crystals in suspension at the end of the experiment, we reduced supersaturation by slightly decreasing NaCl concentration and performed experiment 2: BPTI 20 mg/mL in 1.6 M NaCl and 80 mM sodium acetate buffer solution at pH 4.5, whose supersaturation corresponds to $\beta = 1.4$. We applied a direct voltage of 0.785V and initial current $I_i = 1\mu\text{A}$, which was decreased to 0.6 μA within 15 min, with $t_N \approx 80$ min and $t_{\text{exp}} = 18$ h.

Figure 5a shows the crystallization cell at the end of the experiment. The same trends are observed; namely, nucleation is enhanced and higher near the anode, crystals grow larger near the anode, and a layer is observed around the anode. To check the reversibility of layer formation with polarity, we inverted the polarity of the electrode. Results are presented in Figure 5b–d. The layer starts to dissolve as soon as polarity is inverted. Furthermore, we succeeded in extracting a part of this gel-like layer from the electrode, with titration giving a BPTI concentration of about 900 mg/mL (the accuracy of this measurement is very low ($\pm 50\%$) because the volume of the layer extracted is estimated visually); therefore, this layer is a protein-rich phase. We propose that the formation of this phase is due to a liquid–liquid phase separation (LLPS). LLPS was previously observed for BPTI in KSCN at pH 4.5,^{20,21} but this is the first time to the best of our knowledge that this LLPS has been observed for BPTI in NaCl at pH 4.5. In a previous study,²⁰ we performed scattering experiments on the gel-like state, which proved that BPTI molecules are not aggregated. To confirm that a metastable LLPS occurs in BPTI solution in NaCl at pH 4.5, we performed exploratory experiments by evaporation of a BPTI 20 mg/mL solution in 1.6 M NaCl and 80 mM sodium acetate buffer at pH 4.5; an LLPS was observed. These observations, larger crystals near the anode and LLPS at the anode, suggest a concentration gradient due to the application of the internal direct voltage and to the strong electric field.

Instead of appearing near the cathode (as described in the previous studies on protein crystallization in the presence of an

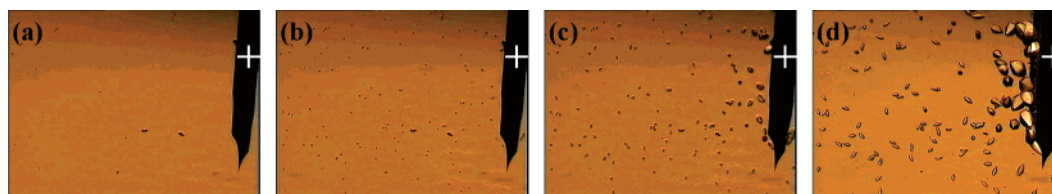


Figure 3. In situ observations under optical microscopy of BPTI crystallization at 20 °C with a direct voltage of 0.785 V (experiment 1), with a time of (a) 0, (b) 7, (c) 11, and (d) 20 h. As reference, the W-electrode wire diameter is 125 μm (the + sign indicates the anode).

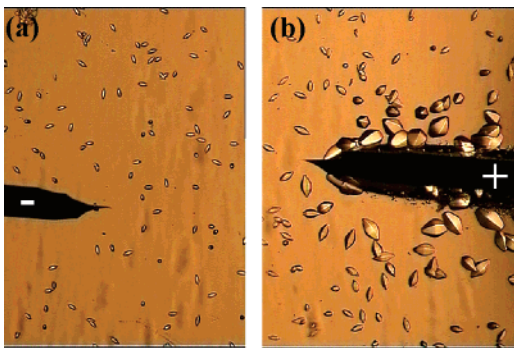


Figure 4. BPTI crystals obtained at 20 °C with a direct voltage of 0.785 V (experiment 1) after 24 h at the (a) cathode and (b) anode. As reference, the W-electrode wire diameter is 125 μm (the + sign indicates the anode).

internal or external electric field⁶) BPTI crystals appeared mainly around the anode.

This result is unexpected because at pH 4.5, monomeric BPTI is positively charged. For BPTI, we showed the coexistence of two different BPTI particles in solution, a monomer and a decamer,²² with the decamer being the growth unit for the acidic BPTI polymorphs;²³ and therefore, the net charge of the BPTI decamer is bound to be different from 10 \times the monomer charge. This is because, in the case of multimeric proteins, some charged residues are accessible and some are buried at the interface. Here, we used a charge of +5 for the monomers and +8 for the decamers obtained when the experimental small-angle X-ray scattering curves were adjusted for supersaturated BPTI solutions at pH 4.5.²¹

The presence in solution of two species of different weights, sizes, and charges may account for this unexpected result, i.e., nucleation at the anode. To confirm this difference, we performed a set of experiments with lysozyme.

3.2. Lysozyme. We performed a set of experiments with lysozyme with the aim of (1) comparing our results with the data from the literature in which lysozyme crystals appeared only around the cathode and (2) testing the effect of having a sharp or rounded electrode. All the experiments were performed under the same conditions: lysozyme 25 mg/mL in 0.7 M NaCl and 80 mM sodium acetate buffer solution at pH 4.5, whose

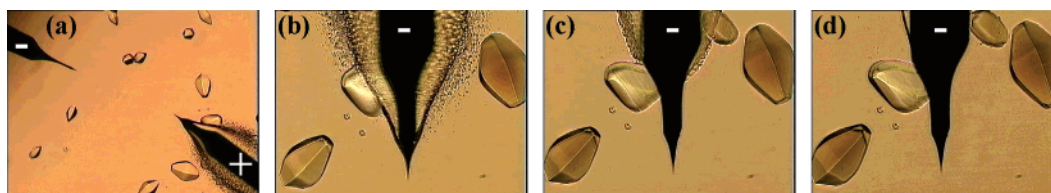


Figure 5. In situ observations under optical microscopy of BPTI crystallization at 20 °C with a direct voltage of 0.785 V (experiment 2), at (a) $t = 18$ h and after inverting the electrode polarity at times of (b) 0, (c) 3.5, and (d) 9 h. As reference, the W-electrode wire diameter is 125 μm (the + sign indicates the anode).



Figure 6. In situ observations under optical microscopy of lysozyme crystallization at 20 °C (lysozyme 25 mg/mL in 0.7 M of NaCl and 50 mM of sodium acetate buffer solution at pH 4.5) with a direct voltage of 0.9 V (experiment 2), at times of (a) 0 and (b) 12 h, and (c) a zoom of the layer formed at the anode. As reference, the W-electrode wire diameter is 125 μm (the + sign indicates the anode).

supersaturation corresponds to $\beta = 5.5$.²⁴ We applied a direct voltage of 0.9 V and initial current $I_1 = 1.3 \mu\text{A}$, $t_N < 1$ h and $t_{\text{exp}} = 12$ h.

In these experiments, summarized in Figure 6, the nucleation is enhanced and higher near the cathode and a layer is observed around the rounded anode. To check whether layer formation depends on polarity and electrode shape, we performed an experiment with the geometry inverted, i.e., with the anode being sharp and the cathode rounded. The layer starts to form at the sharp anode, and crystals appear at the rounded cathode. In addition, we succeeded in extracting a part of this gel-like layer from the electrode, with titration giving a lysozyme concentration of about 900 mg/mL (the accuracy of this measurement is very low ($\pm 50\%$) because the volume of the layer extracted is estimated visually), meaning this layer is a protein-rich phase that visually corresponds to a LLPS (Figure 6c).

We obtained a directed crystallization of the positively charged lysozyme around the cathode. This is mainly due to the polarity of the electrode and not to the strong field region near the sharp tip, as shown by the experiment with the rounded cathode.

So, why does BPTI crystallize at the anode and lysozyme at the cathode even though both are positively charged? Our observations show that the closeness of current lines and the associated high current density at the electrodes appears as a relevant parameter. Therefore, the electromigration of protein in these current lines could govern the crystallization.²⁵ As previously mentioned, the presence of monomer and decamer in the case of BPTI brings an additional complexity. The speed of the electrophoretic motion (SpEM) is proportional to q/r , where q is the charge and r its size.

A numerical application with $r = 14$ and 25 Å for the monomer and decamer sizes,²⁶ respectively, gives a proportionality of 0.36 and 0.32 for the monomer and decamer SpEM. Consequently, the decamer to monomer ratio is not uniform in the solution: it decreases near the cathode and increases near the anode. We showed in a previous paper²² that an increase in this ratio increases the supersaturation, thus enhancing the nucleation (the decamer is the growth unit for acidic BPTI polymorphs). Although that last increase results from the increase of the mean NaCl concentration in a solution at

equilibrium, we anticipate that it is the increase of this ratio that enhances the nucleation at the anode in the present experiment.

4. Conclusions

These results on BPTI and lysozyme crystallizations in the presence of an internal electric field and direct current show that nucleation is enhanced and that crystallization is located near the anode for BPTI and the near cathode for lysozyme.

The crystal size gradient and crystals are larger at the anode for BPTI, which is due to a concentration gradient between the electrodes.

These results are explained using the concept of electromigration of proteins in the electric field.

Thus, preliminary results indicate that this setup takes us closer to controlling the nucleation frequency and the nucleation location. The main problem encountered in nucleation studies and that we address in this study is the unpredictability of the location of the critical nucleus. We expect that with the control of this location, we will be able to better understand the critical nuclei formation. To the best of our knowledge, this has been realized only once by Yau and Vekilov, who were fortunate enough to detect and observe it by a solution AFM cluster after landing on the apoferritin²⁷ crystal surface. The probability of observing such a phenomenon is very low.

Acknowledgment. We thank Bayer A.G. (Wuppertal, Germany) for providing us with BPTI and M. Sweetko for English revision.

References

- (1) Boistelle, R.; Astier, J. P.; Marchis-Mouren, G.; Desseaux, V.; Haser, R. *J. Cryst. Growth* **1992**, *123*, 109–120.
- (2) Astier, J. P.; Veessler, S.; Boistelle, R. *Acta Crystallogr., Sect. D* **1998**, *54*, 703–706.
- (3) Sazaki, G.; Yoshida, E.; Komatsu, H.; Nakada, T.; Miyashita, S.; Watanabe, K. *J. Cryst. Growth* **1997**, *173*, 231–234.
- (4) Taleb, M.; Didierjean, C.; Jelsch, C.; Mangeot, J. P.; Capelle, B.; Aubry, A. *J. Cryst. Growth* **1999**, *200*, 575–582.
- (5) Nanev, C. N.; Penkova, A. *J. Cryst. Growth* **2001**, *232*, 285–293.
- (6) Moreno, A.; Sazaki, G. *J. Cryst. Growth* **2004**, *264*, 438–444.
- (7) Ueno, S.; Ristic, R. I.; Higaki, K.; Sato, K. *J. Phys. Chem. B* **2003**, *107*, 4927–4935.
- (8) Tyndall, J. *Philos. Mag.* **1896**, *37*, 384–394.
- (9) Tam, A.; Moe, G.; Happer, W. *Phys. Rev. Lett.* **1975**, *35*, 1630–1633.
- (10) Garetz, B. A.; Aber, J. E.; Goddard, N. L.; Young, R. G.; Myerson, A. S. *Phys. Rev. Lett.* **1996**, *77*, 3475–3476.
- (11) Zaccaro, J.; Matic, J.; Myerson, A. S.; Garetz, B. A. *Cryst. Growth Des.* **2001**, *1*, 5–8.
- (12) Garetz, B. A.; Matic, J.; Myerson, A. S. *Phys. Rev. Lett.* **2002**, *89*, 175501.
- (13) Okutsu, T.; Nakamura, K.; Haneda, H.; Hiratsuka, H. *Cryst. Growth Des.* **2004**, *4*, 113–115.
- (14) Okutsu, T.; Furuta, K.; Terao, T.; Hiratsuka, H.; Yamano, A.; Ferté, N.; Veessler, S. *Cryst. Growth Des.* **2005**, *5*, 1393–1398.
- (15) Veessler, S.; Furuta, K.; Horiuchi, H.; Hiratsuka, H.; Ferté, N.; Okutsu, T. *Cryst. Growth Des.* **2006**, *6*, 1631–1635.
- (16) Lafont, S.; Veessler, S.; Astier, J. P.; Boistelle, R. *J. Cryst. Growth* **1994**, *143*, 249–255.
- (17) Muller, E. W.; Tsong, T. T. *Field Ion Microscopy: Principles and Applications*; American Elsevier Publishing Company: New York, 1969.
- (18) Hammadi, Z.; Gauch, M.; Morin, R. *J. Vac. Sci. Technol., B* **1999**, *17*, 1390–1394.
- (19) Nieto-Mendoza, E.; Frontana-Uribe, B. A.; Sazaki, G.; Moreno, A. *J. Cryst. Growth* **2005**, *275*, e1437–e1446.
- (20) Grouazel, S.; Perez, J.; Astier, J.-P.; Bonneté, F.; Veessler, S. *Acta Crystallogr., Sect. D* **2002**, *58*, 1560–1563.
- (21) Grouazel, S.; Bonneté, F.; Astier, J.-P.; Ferté, N.; Perez, J.; Veessler, S. *J. Phys. Chem. B* **2006**, *110*, 19664–19670.
- (22) Hamiaux, C.; Perez, J.; Prangé, T.; Veessler, S.; Ries-Kautt, M.; Vachette, P. *J. Mol. Biol.* **2000**, *297*, 697–712.
- (23) Bonneté, F.; Ferté, N.; Astier, J. P.; Veessler, S. *J. Phys. IV* **2004**, *118*, 3–13.
- (24) Ries-Kautt, M. M.; Ducruix, A. F. *J. Biol. Chem.* **1989**, *264*, 745–748.
- (25) Sazaki, G.; Moreno, A.; Nakajima, K. *J. Cryst. Growth* **2004**, *262*, 499–502.
- (26) Grouazel S. *Transition de Phase Liquide-Liquide, interactions en solution et cristallisation dans le cas du BPTI*; Université Aix-Marseille II, Marseille, France, 2005.
- (27) Yau, S. T.; Vekilov, P. G. *Nature* **2000**, *406*, 494–497.

CG070108R